

1 *Influence of temperature on the curing of an epoxy adhesive and its influence*  
2 *on bond behaviour of NSM-CFRP systems*

3

4 Andrea Benedetti<sup>a</sup>, Pedro Fernandes<sup>a</sup>, José L. Granja<sup>a</sup>, José Sena-Cruz<sup>a1</sup>, Miguel Azenha<sup>a</sup>

5

6 <sup>a</sup>ISISE – Institute for Sustainability and Innovation in Structural Engineering

7 University of Minho, School of Engineering

8 Department of Civil Engineering

9 Campus de Azurém

10 4800-058 Guimarães

11 Portugal

12 Tel: +351 253 510 200; Fax: +351 253 510 217

13

14 **ABSTRACT**

15 In NSM-CFRP installations, the mechanical behaviour of the strengthening system is strongly  
16 influenced by the epoxy adhesive, particularly at early ages. In the present work, the influence of  
17 temperature on the curing process of the epoxy was investigated. Three distinct temperatures were  
18 studied: 20, 30 and 40 °C. The elastic modulus of the adhesive was monitored through EMM-ARM  
19 (Elasticity Modulus Monitoring through Ambient Response Method). Direct pull-out tests with concrete  
20 specimens strengthened with NSM CFRP strips were carried out at the same three distinct temperatures  
21 to compare the evolution of bond performance with the E-modulus of epoxy since early ages. The results  
22 showed that increasing the curing temperature significantly accelerated both the curing process of the  
23 epoxy adhesive and the evolution of bond performance. The EMM-ARM technique has revealed its  
24 ability in clearly identifying the hardening kinetics of epoxy adhesives, allowing also thermal activation

---

<sup>1</sup> Corresponding author: [jsena@civil.uminho.pt](mailto:jsena@civil.uminho.pt)

1 analysis. Finally, existing models for predicting temperature-dependent mechanical properties were  
2 extended to also describe the bond behaviour of NSM-CFRP applications.

3

4 **KEYWORDS**

5 A. Carbon fibre

6 A. Thermosetting resin

7 B. Cure behaviour

8 D. Non-destructive testing

9 Near-surface mounted reinforcement

## 1    **1    INTRODUCTION**

2    The potential of near-surface mounted (NSM) technique using carbon fibre reinforced polymers (CFRP)  
3    for strengthening reinforced concrete (RC) structures has been shown in many studies and practical  
4    applications [1-5]. Compared to externally bonded reinforcement (EBR), the NSM system presents  
5    considerable advantages, such as: larger bond surface induces better anchorage capacity [6]; no  
6    preparation work is needed other than grooving; the FRP reinforcement, due to the cover of the  
7    surrounding concrete, has an improved protection against environmental effects, such as freeze/thaw  
8    cycles, elevated temperatures, fire, and vandalism [7, 8]; less prone to premature debonding due to the  
9    larger bonded area and the confinement effect of the grooves, allowing a more efficient use of the  
10    reinforcement material. Although a large number of experimental investigations has been carried out on  
11    the structural behaviour of NSM FRP strengthened RC structures [3, 4], the effect of the curing  
12    conditions on the development of the bond performance is one of the less investigated issues.

13    It is largely acknowledged that the bond performance of NSM-FRP systems is mainly governed by the  
14    mechanical properties of the groove filler [4, 9]. The most employed groove fillers in NSM-FRP systems  
15    are two-component epoxy resin-based adhesives [3, 4]. The chemical reactions that occur during the  
16    curing period are known to be exothermic and transform the two liquid components of the adhesive to  
17    a highly cross-linked space framework by means of polymerization [10]. The parameter that represents  
18    the sensitivity of the reaction rate to temperature is the activation energy. This term is defined as the  
19    thermal energy required to start the chemical reaction [11] and has to be experimentally determined.

20    As the polymerization reactions proceed, the material gradually transforms into a rigid solid glass with  
21    relevant mechanical properties. Previous investigations indicate that the evolution of the tensile  
22    properties (both strength and stiffness) of structural epoxy adhesives strongly depend on the curing  
23    temperature [12-15]. Lower curing temperatures considerably decelerate the process and consequently  
24    the rate of development of mechanical properties [12-15]. However, the works mentioned above were  
25    focused mainly on the adhesive. Only a few investigations were found to be aimed at describing the  
26    evolution of the interface behaviour between FRP and concrete (and not only the adhesive) under various  
27    distinct curing conditions. Dutta and Mosallam [16] studied the strengths of various adhesive bonds  
28    between FRP and concrete under different curing temperatures and durations by means of a field bond

1 strength measuring system. Czaderski et al. [17] carried out pull-off bond tests on externally bonded  
2 CFRP strips glued on concrete at various curing conditions.

3 Both cited works reached similar conclusions: the time development of strength of an adhesive bond is  
4 entirely dependent on curing time and temperature. As both time and temperature increase, the epoxy  
5 bond strength increases. Although all experimental observations pointed out the influence of the curing  
6 conditions on the development of the mechanical parameters, no formulations have been proposed so  
7 far for expressing the relationship between the bond performance at a certain instant in time and the  
8 curing condition. In this context, quantifying the effect of curing temperature and age on the  
9 development of mechanical properties of structural epoxy resins could significantly improve the quality  
10 of the preparation and installation procedures for the strengthening applications.

11 To bridge this gap, the present research focused on two different types of tests, carried out at three  
12 distinct temperatures: 20, 30 and 40 °C. On one hand, EMM-ARM (Elasticity Modulus Measurement  
13 through Ambient Response Method) tests were performed on samples of epoxy resin cured at the  
14 mentioned temperatures with the objective of describing the evolution of the adhesive stiffness since  
15 early ages. The EMM-ARM is a variant of classic resonant frequency methods which allows continuous  
16 E-modulus measurements, and was already used for concrete [18], cement pastes, mortars [19], and  
17 cement-stabilized soils [20]. After the encouraging results obtained in the first applications of EMM-  
18 ARM to epoxy adhesives [21, 22], the present work extends the capability of the methodology to thermal  
19 activation testing. Concomitantly, direct pull-out tests were carried out on CFRP strips embedded in  
20 concrete blocks and cured at different temperatures, for investigation of how the  
21 concrete/adhesive/CFRP bond system is influenced by the curing conditions. A comparison between the  
22 evolution of epoxy E-modulus and the maximum pull-out force was performed, evaluating the  
23 possibility of a correlation between these two entities. Finally, different existing analytical models were  
24 extended for describing the development of the temperature-depended mechanical properties of both the  
25 adhesive and the CFRP-to-concrete interface.

26

## 1    2    **EXPERIMENTAL PROGRAM**

2    In order to characterize the influence of temperature on the curing process of the epoxy adhesive and its  
3    impact on the bond behaviour of NSM-FRP strips, three testing temperatures were considered: 20, 30,  
4    and 40 °C. The experimental program, globally presented in Table 1, can be subdivided into the  
5    following groups of tests:

- 6    (i)    EMM-ARM tests on adhesive samples to assess the evolution of the adhesive elastic  
7    modulus of the epoxy at different curing temperatures;
- 8    (ii)   direct pull-out tests on concrete cubic specimens strengthened with CFRP laminate strips,  
9    aimed at describing the development of the interface behaviour under variable curing  
10    conditions;
- 11    (iii)   tensile tests performed according to EN ISO 527-2:2012 [23], in order to evaluate the  
12    E-modulus value of the hardened epoxy.

13    A specific denomination was devised for the test specimens, each one being labelled as X<sub>n</sub>\_Y\_Z, where  
14    X is the test type (EMM – EMM-ARM test, DPT – direct pull-out test, TT – monotonic tensile test), n  
15    is the specimen number within the series, Y is the testing time (in hours or days), and Z corresponds to  
16    the test temperature. It is noted that EMM-ARM testing provides continuous results, thus the Y  
17    parameter is omitted in the labelling of EMM-ARM test specimens.

18    A single batch of adhesive mixture (with a volume of ~0.9 litres) was made for all the specimens of each  
19    curing temperature, in order to avoid the variability that normally exists between different batches [21].

20    Moreover, it should be noted that the mixing procedures took place in laboratory environment (with  
21    temperature of 20±1 °C) and all the tests were performed at the same respective curing temperature.

22    The whole mixing procedure lasted about 4 min and the instant t = 0 was defined as the moment when  
23    the epoxy components started to be mixed.

24

### 25    **2.1    Materials**

26    Four concrete cylindrical cores with a diameter of 100 mm and a height of 200 mm were used to obtain  
27    the compressive strength and the elastic modulus of concrete used in the pull-out specimens, in  
28    accordance to EN 12390-3:2009 [24] and LNEC E397-1993:1993 [25], respectively. An average

1 compressive strength,  $f_{cm}$ , of 42.35 MPa, with a coefficient of variation CoV of 5.22%, and an average  
2 Young's modulus,  $E_{cm}$ , of 38.25 GPa (CoV=8.38%) were obtained at the age of the experimental  
3 program (approximately three years after concrete casting). The CFRP strips and the epoxy resin were  
4 provided by S&P® Clever Reinforcement. The CFRP strip was the 'CFK 150/2000', with a nominal  
5 thickness of 1.4 mm and a width of 10.0 mm. This laminate is composed of unidirectional fibres in a  
6 vinylester matrix and presents a smooth surface. From six uniaxial tensile tests carried out according to  
7 ISO 527-5:2009 [26] recommendations, the following properties were obtained: Young's modulus equal  
8 to 169.5 GPa (CoV=2.5%), tensile strength equal to 2650 MPa (CoV=1.8%), and ultimate strain equal  
9 to 1.6% (CoV=1.8%).

10 All experimental tests were performed with a commercially available epoxy adhesive termed 'S&P  
11 Resin 220'. This two-component epoxy resin-based adhesive is employed for structural bonding  
12 between FRP composite and concrete or steel and is composed of two parts (Part A = resin and part B  
13 = hardener). According to the material safety data sheets [27, 28], the resin contains Bisphenol A and  
14 neopentyl glycol diglycidyl ether, while the hardener is composed of poly(oxypropylene)diamine,  
15 piperazine, 3,6-diazaoctanethylenediamin and triethylenetetramine. Components A and B are mixed at  
16 a ratio of 4:1 by weight. According to the manufacturer's product guide specification [29], the modulus  
17 of elasticity of the adhesive after 3 days of curing at 20 °C, is larger than 7.10 GPa and the bond strength  
18 on concrete is 3 MPa.

19

## 20 **2.2 EMM-ARM tests**

21 The EMM-ARM is a variant of the traditional resonance frequency methods that allows the measuring  
22 of the material E-modulus since mixing and was already adapted for the study of epoxy adhesives by  
23 Granja et al. [21]. This method is based on the identification of the first resonance frequency of a  
24 cantilever composite beam filled with the material to be tested. The beam is composed by a 330 mm  
25 acrylic tube with external and internal diameters of 20 mm and 16 mm, respectively (see Figure 1). In  
26 one of the extremities, a custom made clamping device is attached to the composite beam, in order to  
27 ensure the structural system, which is a cantilever with a span of 250 mm.

1 In order to identify the natural frequency of the beam, a lightweight accelerometer (mass: 5.8 g;  
2 sensitivity: 100 mV/g; frequency range: 0.5 to 10000 Hz) is attached to the free end of the cantilever  
3 beam that is solely excited by the ambient excitations (e.g., people walking nearby; room ventilation;  
4 vibrations produced by mechanical equipment). However, in order to increase the intensity of the  
5 ambient noise, a fan is placed in the vicinity of the beam. Based on the vertical accelerations measured,  
6 and by means of the Welch procedure [30] (using sub-sets of data with 4096 points (NFFT), Hanning  
7 windows with 50% overlap) and a peak picking method [31], the resonance frequency is identified  
8 through the peak with highest intensity in the power spectrum density. The measured accelerations were  
9 acquired in a 24-bit data logger (NI-USB-9233) with a frequency of 500 Hz, and divided into sets of 5  
10 minutes every 10 minutes. The monitoring procedures started immediately after the correct placement  
11 of all components, which occurred within ~20 min after mixing the epoxy adhesive. After the modal  
12 identification of the first flexural resonance frequency, the rigidity of the composite beam can be  
13 analytically correlated to its frequency through the dynamic equations of the cantilevered structural  
14 system. The whole set of equations used for the characterization of E-modulus is explained in [19]. The  
15 final solution is the differential equation shown below:

$$a^3 \left[ \cosh(a \cdot L) \cdot \cos(a \cdot L) + 1 \right] + \frac{w^2 \cdot m_p}{EI} \left[ \cos(a \cdot L) \cdot \sinh(a \cdot L) - \cosh(a \cdot L) \cdot \sin(a \cdot L) \right] = 0 \quad (1)$$

16 where  $a = \sqrt[4]{w^2 \times \bar{m}/EI}$ ,  $EI$  corresponds to the distributed flexural stiffness of the composite beam,  $\bar{m}$   
17 is the uniformly distributed mass per unit length,  $m_p$  is the concentrated mass at the free extremity of the  
18 cantilever,  $L$  is the span of the cantilever,  $f$  is the first flexural resonant frequency, and  $w = 2\pi f$  is the  
19 corresponding angular frequency.

20 Therefore, for each identified resonant frequency,  $f$ , it is possible to obtain the corresponding  $EI$  of the  
21 composite beam, and since the acrylic E-modulus  $E_a$  is known, the Young modulus of the tested epoxy  
22 adhesive  $E_e$  can be estimated through the equation:

$$EI = E_a \frac{\pi(\varphi_e^4 - \varphi_i^4)}{64} + E_e \frac{\pi\varphi_i^4}{64} \quad (2)$$

1 where  $\varphi_e$  and  $\varphi_i$  are the outer and inner diameters, respectively. In this way, it is possible to relate the  
2 first natural frequency of the composite beam with the elastic modulus of the tested epoxy during the  
3 testing time. As in this work it was intended to perform EMM-ARM measurements at different  
4 temperatures, the E-Modulus of the acrylic mould was accessed before each test at the testing  
5 temperature through modal identification of the empty acrylic tubes [32], following the same protocol  
6 presented before. In order to check the method's ability to obtain results with good repeatability, two  
7 tests were performed simultaneously.

8

### 9 **2.3 Pull-out tests**

10 As previously referred, in order to assess the evolution of bond behaviour of concrete elements  
11 strengthened with NSM-CFRP systems during the hardening of the epoxy adhesive under different  
12 curing temperatures, thirty monotonic direct pull-out tests were carried out for the specific ages (see  
13 Table 1). Figure 2 shows the specimen geometry and the test configuration adopted for the monotonic  
14 direct pull-out tests. The specimen consisted of a concrete cubic block of 200 mm edge, into which a  
15 NSM-CFRP laminate strip with 1.4 mm thickness and 10 mm width was inserted. The strengthening  
16 detail and a cross-section of the groove are presented in Figure 2a. The groove was performed with a fix  
17 saw cut machine. A constant bond length,  $L_b$  of 60 mm, filled with the epoxy adhesive was adopted. The  
18 justification for such fixed value of the bond length can be found elsewhere [33]. To avoid premature  
19 splitting in the concrete ahead the loaded end, the bond length started 100 mm far from the top of the  
20 block. To assure negligible vertical displacement at the top of the concrete specimen during pull-out  
21 test, a steel plate with 20 mm thickness was applied at the top of the concrete block. This plate was fixed  
22 to the support base through four M10 steel threaded rods. A torque of 30 N×m was applied, inducing an  
23 initial compression to concrete of about 2.0 MPa. The pull-out tests were performed on a closed steel  
24 frame equipped with a servo-controlled equipment. As previously mentioned, the testing temperature  
25 was the same as that of the corresponding curing. For this purpose, a custom-made temperature chamber  
26 was manufactured with Expanded Polystyrene plates (see Figure 2b). A heater was placed inside a  
27 climatic chamber and an automatic system (thermostat equipped with a platinum resistor thermometer

1 (PT100) sensor) was used to control the imposed temperature. Additionally, a thermocouple type k was  
2 placed near to the bond region.

3 A LVDT (range  $\pm 2.5$  mm with a linearity error of  $\pm 0.05\%$  F.S.) was used to measure the slip at the  
4 loaded end,  $s_l$ . The applied force,  $F$ , was registered by a load cell of 200 kN of capacity (with a linearity  
5 error less than  $\pm 0.05\%$  F.S.) placed between the load actuator and the grip. The tests were performed  
6 under displacement control at a rate of  $2 \mu\text{m/s}$ , assessed by another LVDT placed between the actuator  
7 and the grip. Before strengthening, several measurements were carried out for each specimen to assess  
8 the actual geometry of the grooves, using a digital calliper with an accuracy of  $\pm 0.01$  mm (see Table 2).  
9 The strengthening of the specimens was carried out when the grooves were completely dry and clean.  
10 The strengthening was performed at laboratory environment ( $T=21\pm 2$  °C) for all the studied  
11 temperatures. Afterwards, the specimens were put into the previously described temperature chamber  
12 (which occurred within  $\sim 20$  min since the epoxy components started to be mixed) and were kept under  
13 controlled temperature until the age of testing. It is important to remark that, before the strengthening  
14 procedure, the adhesive epoxy was kept in the climatic chamber at  $T=20\pm 1$  °C and  $\text{RH}=60\pm 5\%$ . Detailed  
15 description about the specimen preparation and strengthening procedure can be found elsewhere [33].

16

### 17 **3 RESULTS AND DISCUSSION**

#### 18 **3.1 Epoxy E-modulus**

19 The development of the epoxy E-moduli obtained through EMM-ARM at the three curing temperatures  
20 under test (20, 30 and 40 °C) are presented in Figure 3a. The results of tensile tests are shown in Figure  
21 4 and also added to the Figure 3a. The modulus of elasticity was calculated from tensile test results  
22 based on the highest slope of the stress-strain curve, in accordance with the work of Moussa et al. [34].  
23 Observation of EMM-ARM results in Figure 3a allows verifying that the E-modulus curves  
24 corresponding to the same temperature have very good coherence with each other, with absolute  
25 stiffness differences under 3.0% at all instants ( $\sim 0.27$  GPa at the age of 144 hours at 20 °C),  
26 demonstrating adequate repeatability of EMM-ARM. Furthermore, there is a good agreement between  
27 the E-Modulus estimated through the EMM-ARM and the tensile tests, with stiffness differences under  
28 3.2% ( $\sim 0.31$  GPa for the 40 °C test).

1 In addition, the results show that the reaction rates intensify with the increase of the curing temperature,  
2 since it can be observed that, for example, the elastic modulus of 4 GPa is achieved at approximately  
3 10.7 hours at 20 °C as opposed to the approximately 6.2 and 5.5 hours at 30 and 40°C, respectively.  
4 These variations also occur in the duration of the dormant period. With the increase in the curing  
5 temperature the duration of the dormant period becomes shorter, as can be observed in the Figure 3b.  
6 At the reference temperature (20 °C) the setting time (herein defined as the time when the E-Modulus  
7 reached 0.25 GPa) was  $4.5\pm 0.2$  hours, as opposed to the shorter 2.6 hours observed in the test at 40 °C.  
8 It should also be noted that the E-Modulus of the epoxy at 144 hours increased slightly with the increase  
9 of the curing temperature, reaching final values of 8.9, 9.3 and 9.5 for the tests at 20, 30 and 40 °C,  
10 respectively, in accordance with observations made by several previous works on epoxy adhesives [34-  
11 36]. This phenomenon can be mainly attributed to a higher cross-link density formation of the epoxy  
12 resin cured at higher temperatures. Typically, higher temperatures produce a more complete reaction  
13 with a greater degree of cross-linking than lower temperatures, providing sufficient kinetic energy to  
14 quickly initiate chemical reactions at even the most hindered locations [36]. It is well-known that  
15 increasing the cross-link density leads to improvements in the mechanical properties of epoxy polymers  
16 [37-39].

17

### 18 **3.2 Pull-out force**

19 The main results of the monotonic pull-out tests are summarized in Table 3. In order to assess the  
20 evolution of bond performance, the following parameters were analysed: the maximum pull-out force,  
21  $F_{l,max}$ ; the slip at the loaded end at  $F_{l,max}$ ,  $s_{l,max}$ ; the average bond strength at the CFRP-epoxy interface,  
22  $\tau_{max}$  that is evaluated by the expression  $F_{l,max}/(P_f L_b)$ , where  $P_f$  is the perimeter of the CFRP cross-section  
23 in contact with the adhesive and  $L_b$  is the bond length. Table 3 also provides information about the  
24 failure mode of the tested specimens, with the following codes: D=debonding at CFRP-epoxy interface;  
25 FE=cohesive shear failure in epoxy; CC=concrete cracking; SE=splitting of epoxy.

26 The relationship between the pull-out force and slip at loaded end ( $F_l - s_l$ ) for all tested specimens at  
27 three different temperatures (20, 30 and 40 °C) of curing are presented in Figures 5a, b and c. It is  
28 possible to observe the increase on bond stiffness along the curing of epoxy adhesive. This evolution

1 process seems to be totally governed by the state of hardening of the adhesive. The process of hardening  
2 depends on the curing temperature, as can be seen in the Figure 5. At 20 °C the pull-out force remains  
3 approximately zero at the age of 6 hours, since the epoxy has not yet begun to harden. On the other hand,  
4 at the same testing age, the maximum pull-out forces of 5.36 kN and 10.46 kN are achieved at 30 and  
5 40 °C, respectively. According to the obtained results for 20 and 30 °C, the authors decided to perform  
6 a pull-out test at 40 °C for the age of 4 hours. As can be seen in Figure 5c, at the age of 4 hours, the  
7 epoxy has already begun to harden, with a maximum pull-out force of 2.6 kN.

8 For the three analysed temperatures, the bond stiffness had a significant increase from 6 to 24 hours,  
9 showed by the sharp slope difference of the curves obtained by the tests performed between 6 and 24  
10 hours. However, for 40 °C, at 12 hours the  $F_l - s_l$  response exhibit the bond-slip behaviour similar for  
11 ages higher than 24 hours, when the epoxy has achieved a significant maturity level. In general, after  
12 the first 24 hours the bond stiffness did not show any significant variation. In terms of average maximum  
13 pull-out force considering the specimens tested at 72 hours at 30 °C and 40 °C the values were very close  
14 ( $27.79 \pm 0.03$  kN) and were higher (9.2 % on average) than those of 20 °C, that is consistent with the  
15 obtained final values of epoxy E-modulus (see Figure 3a).

16 Regarding to the failure modes, it is possible to observe that at the early ages until ~12 hours the failure  
17 mode tend to be cohesive and occurring in the adhesive by shear failure (FE), as Table 3 shows,  
18 confirming the low mechanical properties of the adhesive at the beginning of the curing. This type of  
19 failure mode has been also reported and observed by other researchers e.g. [40, 41]. Furthermore, in  
20 some specimens, the performed tests also led to cracking of the epoxy cover and fracture in the concrete  
21 along inclined planes (at ~72 hours for 20 °C and at 24 and 72 hours for 40 °C).

22 It is important to underline that for high pull-out forces (~25 kN), for the test temperatures T30 and T40  
23 the failure mode still occurs by shear failure (cohesive in epoxy), when compared to the test temperature  
24 T20, where this type of failure mode only happens for low values of pull-out force (~14 kN). These  
25 results indicate that the temperature of curing plays a key role on a global behaviour.

26 For the description of the pull-out test results, a fitting equation based on the one proposed by Silva,  
27 Azenha [20] in the context of E-modulus predictions was used. The proposed equation expresses the  
28 evolution of pull-out force according to:

$$F(t) = F_{ult} \exp\left[-\frac{1}{2}\left(\frac{\lambda}{t}\right)^\beta\right] \quad (3)$$

1 where  $F_{ult}$  is the average of experimental values for the specimens tested from 72 hours;  $\beta$  is the reaction  
 2 shape parameter and  $\lambda$  is the reaction time parameter. This model was applied in order to use the methods  
 3 for obtaining the activation energy that will be shown in the next section. Regression analyses were  
 4 performed to determine these parameters, using experimental values (see Table 4). The best fit was  
 5 achieved using the method of least squares, in order to maximize the coefficient of determination  
 6 between the model and the experimental curve. By observing Figure 6 it is possible to verify that the  
 7 use of Equation (3) allows to obtain a very good estimate of pull-out force evolution ( $0.969 \leq R^2 \leq$   
 8  $0.982$ ), even at the early stages of the curing.

9 Finally, it should be noted that  $F_{ult}$  is variable with temperature. This happens because the failure modes  
 10 occurred in the pullout tests were governed by the mechanical properties of the adhesive (see Table 3),  
 11 which are improved by increased curing temperatures (in the range tested here). Similar behaviours have  
 12 also been observed and reported by previous research works [42]. It is however noted that, according to  
 13 the literature [43], for the cases where the failure is cohesive within the concrete, the maximum load  
 14 carrying capacity of NSM-CFRP concrete systems are not affected by the curing temperature (in the  
 15 range tested here).

### 17 3.3 Relationship between pull-out force and E-modulus

18 With the purpose of evaluating the possibility of a correlation between the interface behaviour of NSM  
 19 systems and the epoxy stiffness, a comparison between the peak pull-out force and the adhesive E-  
 20 modulus is carried out for the three studied temperatures, as shown in Figure 7. In order to compare  
 21 better the results pertaining to different temperatures, all the values were normalized in regard to the  
 22 measurements obtained at the age of 72 hours. Figure 7a highlights that the peak pull-out force and the  
 23 epoxy E-modulus obtained by EMM-ARM exhibit very similar evolution kinetics, thus indicating that  
 24 the bond performance of NSM CFRP system strongly depends on the stiffness of the adhesive regardless  
 25 of the curing temperature. The increase on bond stiffness is consistent with the stage at which the rate

1 of thermosetting reactions is higher, although its development was slightly delayed compared to E-  
2 modulus development. During the analysis of the results, the authors also analysed the possibility of  
3 correlating bond stiffness obtained from the pullout tests and elastic modulus of the epoxy adhesive.  
4 However, due to the high dispersion obtained in this correlation along the curing time, the comparison  
5 between both parameters was unfeasible, and the authors decided not to include it herein. As opposed,  
6 the correlation between elastic modulus and maximum pull-out force is valid taking into account the  
7 observed failure modes, which are governed by the mechanical properties of the epoxy adhesive and/or  
8 the mechanisms of adhesion between CFRP and epoxy (cohesive in epoxy and debonding at CFRP-  
9 epoxy interface). Figure 7b illustrates the relationship between the E-modulus of the epoxy-resin and  
10 the maximum pull-out force for the different curing temperatures: the scatter in the measured properties  
11 tended to be highest when the slope of the curves in Figure 7a was steepest and then decreased for later  
12 ages. The slight difference on the kinetics of the two properties seems to be similar for all temperatures  
13 and may be attributed to a delay in the development of the molecular bond quality, which usually has  
14 less influence on the stiffness of the epoxy resin than on its strength [12]. Based on this kind of  
15 relationship, EMM-ARM can be employed for estimating the maximum pull-out force and the minimum  
16 curing time to reach a threshold value of pull-out force. In this manner it is possible to know the time  
17 required to put the strengthened structure in service, taking into account the influence of different  
18 environmental curing conditions.

19

#### 20 **4 KINETIC MODELLING**

21 A kinetic analysis is presented in the following paragraphs to describe the experimental results of both  
22 the adhesive E-modulus and pull-out force. Two different approaches were considered for the kinetic  
23 analysis. The first approach was based on fitting the experimental data to an assumed reaction model,  
24 better known as phenomenological model [44]. The data was fitted to a single-step reaction model that  
25 yields a single averaged value of the activation energy for the overall cure process. An alternative  
26 approach to the phenomenological model is the model-free isoconversional method [45] , also used in  
27 the present work. Without assuming a particular form of the reaction model, this latter method allows  
28 evaluating the effective activation energy as a function of the extent of the cure. The activation energy

1 can be considered a time-temperature shift factor and as such it is useful in predicting the time to reach  
 2 a specific curing degree as a function of temperature. This concept, well-known as time-temperature  
 3 superposition [46], can be expressed by a relationship which relates the times to reach a certain  
 4 conversion at two different temperatures ( $T_{cure}$  and  $T_{ref}$ ). Prime [47] proposed the following  
 5 isoconversion Arrhenius relationship:

$$t_{eq} = \sum_0^t \exp \left[ \frac{E_a (T_{cure} - T_{ref})}{R T_{ref} T_{cure}} \right] \cdot \Delta t \quad (4)$$

6 Where  $t$  is the instant at which the equivalent age is being computed,  $t_{eq}$  is the equivalent age at the  
 7 reference temperature  $T_{ref}$ ,  $T_{cure}$  is the temperature of cure,  $E_a$  is the activation energy, and  $R$  is the gas  
 8 constant (8.314 kJ/mol·K). Therefore, a time-temperature shifting was performed using the activation  
 9 energy calculated for both phenomenological model and isoconversional method, thus allowing a  
 10 comparison between the two different methods.

11

#### 12 **4.1 Autocatalytic model**

13 In the context of curing process of different materials the autocatalytic model has a widespread  
 14 acceptance and is typically used. The curing reaction can be described by a rate equation given by the  
 15 following expression [48]:

$$\frac{d\alpha}{dt} = k(T)f(\alpha) \quad (5)$$

16 where  $\alpha$  is the curing degree,  $d\alpha/dt$  is the curing rate,  $T$  is absolute temperature (in K),  $k(T)$  is the rate  
 17 constant, and  $f(\alpha)$  is the function that describes the curing reaction mechanism. Here, the curing degree  
 18 is quantified as follows:

$$\alpha(t) = \frac{E(t)}{E_{ult}} \quad (6)$$

19  $E(t)$ ,  $E_{ult}$ : monitored E-modulus of epoxy resin at age  $t$ , and E-modulus at 144 hours. Based on the EMM-  
 20 ARM results, a kinetic model of autocatalytic curing reactions was assumed [46], namely:

$$f(\alpha) = \alpha^m (1 - \alpha)^n \quad (7)$$

1 where  $m$  and  $n$  are the reaction orders independent of temperature, and  $\alpha^m$  represents the catalytic effect.  
 2 This function exhibits a delayed cure rate peak, which occurs during the curing process, while at the  
 3 beginning of the reaction ( $t = 0$ ), the term curing rate,  $da/dt$ , is zero for all temperatures. The reaction  
 4 parameters  $k$ ,  $m$  and  $n$  were obtained by fitting the isothermal data [49] with the non-linear least square  
 5 regression method based on the Generalized Reduced Gradient algorithm [50]. The relationship between  
 6 the curing rate and the curing degree is shown in Figure 8. Experimental results were satisfactorily  
 7 simulated by the selected autocatalytic model. At 20 °C, the maximum curing rate occurred at a curing  
 8 degree of approximately 25%, while at higher curing temperatures (30 and 40 °C) the curves exhibited  
 9 a lightly delayed peak at around 32% curing degree. The kinetic rate constant  $k$  follows an Arrhenius  
 10 temperature dependence [51]:

$$k(T) = A \exp\left(-\frac{E_a}{RT}\right) \quad (8)$$

11  $A$ : proportionality constant;  $E_a$ : activation energy of epoxy resin (J/mol);  $R$ : gas constant (8.314 kJ/mol  
 12 K). The kinetic rate equation can therefore be rewritten as:

$$\frac{d\alpha}{dt} = f(\alpha) A \exp\left(-\frac{E_a}{RT}\right) \quad (9)$$

13 By plotting the logarithms of the rate constant  $\ln(k)$  versus  $1/T$ , it was possible to obtain both the  
 14 activation energy,  $E_a$ , and the natural logarithm of the pre-exponential factor,  $\ln(A)$ , from the slope and  
 15 the y intercept of a linear fit of the results shown in Figure 9a. Their values, together with the reaction  
 16 parameters, are given in Table 5. The activation energy was determined to be 34.05 kJ/mol. In Figure  
 17 9b the curing degree values are plotted as a function of equivalent age. From this figure, a poor quality  
 18 of the superposition can be visually identified. The fact that the points in Figure 9a are not aligned  
 19 confirms that the autocatalytic model activation energy concept was not effective for describing the  
 20 obtained experimental results, since the activation energy depends on the temperature interval. In fact,  
 21 the obtained value ends up to be an intermediate value.

22

## 1 4.2 Model-free isoconversional method

2 This method is based on the single-step kinetic equation and is founded on the isoconversional principle,  
3 which states that at a constant extent of conversion, the reaction rate is only a function of the temperature  
4 [45]. The Arrhenius equation for two different tests can be described by the following expression:

$$\left(\frac{d\alpha}{dt}\right)_i = f(\alpha_i) A \exp\left(-\frac{E_a}{RT_i}\right) \quad (10)$$

5 where  $i = 1, 2$  represents each of the two tests. By taking the same fixed value of the curing degree ( $\alpha_1$   
6  $= \alpha_2$ ) and dividing one equation by the other yields:

$$\left(\frac{d\alpha}{dt}\right)_1 = \left(\frac{d\alpha}{dt}\right)_2 \exp\left(-\frac{E_a}{R}\left(\frac{1}{T_1} - \frac{1}{T_2}\right)\right) \quad (11)$$

7 Thus, for each value of the curing degree  $\alpha$ , a corresponding model-free value of the activation energy  
8 is obtained:

$$E_a(\alpha) = -\frac{R}{T_1 - T_2} \ln \frac{\left(\frac{d\alpha}{dt}\right)_1}{\left(\frac{d\alpha}{dt}\right)_2} \quad (12)$$

9 This method allows calculation of the activation energy from two different tests, and does not require  
10 any information about the cure mechanism. However, this equation gives no indication about the  
11 reaction order and Arrhenius pre-exponential factor. The analysis of experimental results enabled to plot  
12  $E_a$  as a function of the curing degree for each couple of EMM-ARM tests (see Figure 10a). Comparing  
13 the relationship of the curing degree with the equivalent age for both studied models, it is possible to  
14 observe that the isoconversional method leads to better results, i.e. the superposition of the curves for  
15 all the tested specimens, as can be seen in Figure 10b.

16 Taking account of the results obtained for the E-modulus, the same strategy was applied to the pull-out  
17 force only by means of the model-free method. Here, the curing degree is quantified as follows:

$$\alpha(t) = \frac{F(t)}{F_{ult}} \quad (13)$$

18 where  $F(t)$  is the pull-out force at age  $t$  and  $F_{ult}$  is the ultimate pull-out force of the model. The evolution  
19 of the activation energy with the curing degree for the pull-out force is plotted in Figure 11a. The

1 evolution of the  $E_a$  curves presented similar shape in comparison with EMM-ARM specimens. Despite  
2 the similarity of between the activation energy values obtained for the E-modulus and pull-out force  
3 evolutions for the temperatures 20-40 °C (e.g. both around 19.3 kJ/mol at curing degree of 0.5 with  
4 difference of 8.8%), there is a significant difference for the temperatures 20-30 °C the values of the  
5 activation energy exhibit a considerable difference (difference of 28.0% for the curing degree of 0.5).  
6 This fact indicates that the influence of temperature on the activation energy is different in these two  
7 properties. In Figure 11b the pull-out force curves are plotted as a function of equivalent age. It is  
8 possible to confirm the capability of the method to predict the activation energy of both epoxy E-  
9 modulus and pull-out force as a time-temperature shift factor. Therefore it is possible to predict the time  
10 to reach a specific conversion as a function of temperature.

11

## 12 **5 CONCLUSIONS**

13 The present paper presented an experimental study for the evaluation of the influence of temperature on  
14 the curing process of the structural epoxy and its impact on the bond behaviour of NSM-CFRP  
15 strengthening applications. Three distinct temperatures were studied: 20, 30 and 40 °C. The elastic  
16 modulus of the adhesive was continuously monitored through EMM-ARM. Concomitantly, direct pull-  
17 out tests were carried out on CFRP strips embedded in concrete blocks and cured at different  
18 temperatures, in order to investigate how the bond between concrete and NSM-CFRP is influenced by  
19 the curing conditions. A comparison between the evolution of epoxy E-modulus and the maximum pull-  
20 out force was performed, evaluating the possibility of a correlation between these two entities. Finally,  
21 different existing analytical models were extended for describing the kinetic analysis of both the  
22 evolution of E-modulus and the pull-out force. The main conclusions of the study can be summarized  
23 as follows:

- 24 1. EMM-ARM has confirmed its capability to access the E-modulus of epoxies adhesives with  
25 adequate repeatability in accordance to previous works [21, 22], and it further demonstrated  
26 capability to perform studies at temperatures up to 40 °C. The method was also able to assess  
27 the increase of the epoxy stiffness with the increase of the curing and testing temperatures.

- 1        2. The E-modulus results shows that the reaction rates intensify with the increase of the curing  
2            temperature during both the dormant and the hardening periods.
- 3        3. The bond behaviour of NSM-CFRP concrete systems is totally governed by the state of  
4            hardening of the adhesive. The process of hardening depends on the curing temperature. For the  
5            three analysed temperatures, the bond stiffness and maximum pull-out force had a significant  
6            increase from 6 to 24 hours. For 40 °C, after 12 hours of curing the  $F_l - s_l$  response exhibits a  
7            bond-slip behaviour similar to ages when the epoxy can be considered cured. The increase on  
8            bond stiffness and maximum pull-out force are consistent with the stage at which the rate of  
9            thermosetting reactions is higher, although its development was slightly delayed compared to  
10          E-modulus development. In general, after the first 24 hours the bond stiffness and bond strength  
11          did not show any significant variation.
- 12       4. In terms of failures modes, the failure mode was cohesive in the adhesive due to the low  
13          mechanical properties of the adhesive at the beginning of the curing, and after certain curing  
14          degree the failure mode changed from cohesive shear failure in epoxy to debonding at CFRP-  
15          epoxy interface. However, the transition point changed with curing temperature, i.e. increasing  
16          the curing temperature, the transition occurs at higher values of pull-out force (e.g. for the test  
17          temperatures T20 and T40, the transition point occurs for 14 kN and 23 kN, respectively).
- 18       5. The results obtained through EMM-ARM allowed the estimation of activation energy evolution  
19          throughout the whole epoxy curing process by application of the model-free isoconversional  
20          method. This model has further shown adequate performance to estimate the activation energy  
21          of pull-out force as a time-temperature shift factor when compared to the autocatalytic model.
- 22       6. Despite the fact that the autocatalytic model has a widespread acceptance, being typically used  
23          in similar contexts, for the present case it turned out to perform poorly for describing the  
24          obtained experimental results, since the activation energy depends on the curing temperature.
- 25       7. The evolution of the activation energy presented similar shape between the E-modulus and pull-  
26          out force. Furthermore the activation energy exhibits a significant temperature dependence, i.e.  
27          increasing the curing temperature the activation energy increase. This dependency was also  
28          different for the two evaluated entities (E-modulus and pull-out force).

1 8. Despite the present results being credible, contributing for the knowledge in this area, further  
2 investigation is required to better understand the influence of curing temperature on evolution  
3 kinetic of the mechanical properties of the epoxy adhesive and properties of adhesion between  
4 materials, as well as to confirm the observed tendencies.

## 6 **6 ACKNOWLEDGEMENTS**

7 This work is supported by FEDER funds through the Operational Program for Competitiveness Factors  
8 - COMPETE and National Funds through FCT - Portuguese Foundation for Science and Technology  
9 under the projects FRPreDur FCOMP-01-0124-FEDER-028865 (FCT no. PTDC/ECM-  
10 EST/2424/2012) and VisCoDyn FCOMP-01-0124-FEDER-041751 (FCT no. EXPL/ECM-  
11 EST/1323/2013). The authors also like to thank all the companies that have been involved supporting  
12 and contributing for the development of this study, mainly: S&P Clever Reinforcement Ibérica Lda.,  
13 Artecanter - Indústria de Transformação de Granitos, Lda., Vialam – Indústrias Metalúrgicas e  
14 Metalomecânicas, Lda. The second and third authors also acknowledge the grants  
15 SFRH/BD/80338/2011 and SFRH/BD/80682/2011, respectively, provided by FCT.

16

## 1 REFERENCES

- 2 [1] Rizzo A, De Lorenzis L. Behavior and capacity of RC beams strengthened in shear with NSM FRP  
3 reinforcement. *Construction and Building Materials*. 2009;23(4):1555-67.
- 4 [2] Rizkalla S, Hassan T, Hassan N. Design recommendations for the use of FRP for reinforcement and  
5 strengthening of concrete structures. *Progress in Structural Engineering and Materials*. 2003;5(1):16-28.
- 6 [3] De Lorenzis L, Teng JG. Near-surface mounted FRP reinforcement: An emerging technique for  
7 strengthening structures. *Composites Part B: Engineering*. 2007;38(2):119-43.
- 8 [4] Coelho MRF, Sena-Cruz JM, Neves LAC. A review on the bond behavior of FRP NSM systems in  
9 concrete. *Construction and Building Materials*. 2015(0).
- 10 [5] Garzón-Roca J, Sena-Cruz JM, Fernandes P, Xavier J. Effect of wet-dry cycles on the bond  
11 behaviour of concrete elements strengthened with NSM CFRP laminate strips. *Composite Structures*.  
12 2015;132(0):331-40.
- 13 [6] Sena-Cruz JM, Barros JAO, Coelho MRF, Silva LFFT. Efficiency of different techniques in flexural  
14 strengthening of RC beams under monotonic and fatigue loading. *Construction and Building Materials*.  
15 2012;29(0):175-82.
- 16 [7] Silva P, Fernandes PMG, Sena-Cruz J, Azenha M, Barros JA. Behaviour of concrete elements  
17 strengthened with near surface mounted CFRP strips under thermal cycles. CICE 2014. Vancouver,  
18 Canada 2014.
- 19 [8] Szabó ZK, Balázs GL. Near surface mounted FRP reinforcement for strengthening of concrete  
20 structures. *Civil Engineering*. 2007;51(1):33-8.
- 21 [9] Borchert K, Zilch K. Bond behaviour of NSM FRP strips in service. *Structural Concrete*. 2008;9:127-  
22 42.
- 23 [10] Gillham JK. Formation and properties of thermosetting and high Tg polymeric materials. *Polymer*  
24 *Engineering & Science*. 1986;26(20):1429-33.
- 25 [11] Sbirrazzuoli N, Vyazovkin S. Learning about epoxy cure mechanisms from isoconversional  
26 analysis of DSC data. *Thermochimica Acta*. 2002;388(1):289-98.
- 27 [12] Moussa O, Vassilopoulos AP, de Castro J, Keller T. Early-age tensile properties of structural epoxy  
28 adhesives subjected to low-temperature curing. *International Journal of Adhesion and Adhesives*.  
29 2012;35:9-16.
- 30 [13] Dodiuk H, Kenig S. Low temperature curing epoxies for structural repair. *Progress in Polymer*  
31 *Science*. 1994;19(3):439-67.
- 32 [14] Matsui K. Effects of curing conditions and test temperatures on the strength of adhesive-bonded  
33 joints. *International Journal of Adhesion and Adhesives*. 1990;10(4):277-84.
- 34 [15] Lapique F, Redford K. Curing effects on viscosity and mechanical properties of a commercial  
35 epoxy resin adhesive. *International Journal of Adhesion and Adhesives*. 2002;22(4):337-46.
- 36 [16] Dutta PK, Mosallam A. A rapid field test method to evaluate concrete composite adhesive bonding.  
37 *International Journal of Materials and Product Technology*. 2003;19(1):53-67.
- 38 [17] Czaderski C, Martinelli E, Michels J, Motavalli M. Effect of curing conditions on strength  
39 development in an epoxy resin for structural strengthening. *Composites Part B: Engineering*.  
40 2012;43(2):398-410.
- 41 [18] Azenha M, Magalhães F, Faria R, Cunha Á. Measurement of concrete E-modulus evolution since  
42 casting: A novel method based on ambient vibration. *Cement and Concrete Research*. 2010;40(7):1096-  
43 105.
- 44 [19] Azenha M, Faria R, Magalhães F, Ramos L, Cunha Á. Measurement of the E-modulus of cement  
45 pastes and mortars since casting, using a vibration based technique. *Mater Struct*. 2012;45(1-2):81-92.
- 46 [20] Silva J, Azenha M, Correia AG, Ferreira C. Continuous stiffness assessment of cement-stabilised  
47 soils from early age. *Geotechnique*. 2013;63(16):1419-32.
- 48 [21] Granja JL, Fernandes P, Benedetti A, Azenha M, Sena-Cruz J. Monitoring the early stiffness  
49 development in epoxy adhesives for structural strengthening. *International Journal of Adhesion and*  
50 *Adhesives*. 2015;59:77-85.
- 51 [22] Fernandes P, Granja JL, Benedetti A, Sena-Cruz J, Azenha M. Quality control and monitoring of  
52 NSM CFRP systems: E-modulus evolution of epoxy adhesive and its relation to the pull-out force.  
53 *Composites Part B: Engineering*. 2015;75:95-103.

- 1 [23] ISO. 527-2:2012 Plastics - Determination of tensile properties - Part 2: Test conditions for moulding  
2 and extrusion plastics. Genève, Switzerland: International Organization for Standardization; 2012.
- 3 [24] EN. 12390-3 Testing hardened concrete. Compressive strength of test specimens. Part 3:  
4 Compressive strength of test specimens. BSI; 2009.
- 5 [25] LNEC. E397-1993 Betões – Determinação do módulo de elasticidade em compressão  
6 Documentação Normativa Especificação LNEC [In Portuguese]; 1993.
- 7 [26] ISO. 527-5:2009 Plastics - Determination of tensile properties - Part 5: Test conditions for  
8 unidirectional fibre-reinforced plastic composites. Genève, Switzerland: International Organization for  
9 Standardization; 2009.
- 10 [27] S&P. S&P Resin 220 (Comp A), Safety data sheet. 2013. p. 8.
- 11 [28] S&P. S&P Resin 220 (Comp B), Safety data sheet. 2011. p. 6.
- 12 [29] S&P. S&P Resin 220 epoxy adhesive, Technical Data Sheet. 2013. p. 3.
- 13 [30] Welch PD. The use of fast Fourier transform for the estimation of power spectra: A method based  
14 on time averaging over short, modified periodograms. *Audio and Electroacoustics, IEEE Transactions*  
15 *on.* 1967;15(2):70-3.
- 16 [31] Oppenheim AV, Schaffer RW. *Discrete-Time Signal Processing*: Prentice Hall Press; 2009.
- 17 [32] Granja J, Azenha M, Sousa Cd, Ferreira C. Comparison Between Different Experimental  
18 Techniques for Stiffness Monitoring of Cement Pastes. *Journal of Advanced Concrete Technology.*  
19 2014;12(2):46-61.
- 20 [33] Fernandes PMG, Silva PM, Sena-Cruz J. Bond and flexural behavior of concrete elements  
21 strengthened with NSM CFRP laminate strips under fatigue loading. *Engineering Structures.*  
22 2015;84(0):350-61.
- 23 [34] Moussa O, Vassilopoulos AP, de Castro J, Keller T. Time-temperature dependence of  
24 thermomechanical recovery of cold-curing structural adhesives. *International Journal of Adhesion and*  
25 *Adhesives.* 2012;35:94-101.
- 26 [35] Lionetto F, Maffezzoli A. Monitoring the Cure State of Thermosetting Resins by Ultrasound.  
27 *Materials.* 2013;6(9):3783-804.
- 28 [36] Sun L, Pang S-S, Sterling AM, Negulescu II, Stubblefield MA. Thermal analysis of curing process  
29 of epoxy prepreg. *Journal of Applied Polymer Science.* 2002;83(5):1074-83.
- 30 [37] Shokuhfar A, Arab B. The effect of cross linking density on the mechanical properties and structure  
31 of the epoxy polymers: molecular dynamics simulation. *Journal of molecular modeling.*  
32 2013;19(9):3719-31.
- 33 [38] Ahmad Z, Ansell M, Smedley D. Thermal properties of epoxy-based adhesive reinforced with nano  
34 and micro-particles for in-situ timber bonding. *Int J Eng Technol.* 2010;10(2):32-8.
- 35 [39] Sancaktar E, Jozavi H, Klein RM. The Effects of Cure Temperature and Time on the Bulk Tensile  
36 Properties of a Structural Adhesive. *The Journal of Adhesion.* 1983;15(3-4):241-64.
- 37 [40] Teng J, De Lorenzis L, Wang B, Li R, Wong T, Lam L. Debonding Failures of RC Beams  
38 Strengthened with Near Surface Mounted CFRP Strips. *Journal of Composites for Construction.*  
39 2006;10(2):92-105.
- 40 [41] Blaschko M. Bond behaviour of CFRP strips glued into slits. *Sixth International Symposium on*  
41 *FRP Reinforcement for Concrete Structures (FRPRCS-6)*: World Scientific; 2003. p. 8-10.
- 42 [42] Palmieri A, Matthys S, Taerwe L. Influence of High Temperature on Bond between NSM FRP  
43 Bars/Strips and Concrete. *ACI Special Publication.* 2011;275:1-12.
- 44 [43] Klamer EL, Hordijk DA, Hermes MC. The influence of temperature on RC beams strengthened  
45 with externally bonded CFRP reinforcement. *Heron.* 2008;53(3):157-85.
- 46 [44] Yousefi A, Lafleur P, Gauvin R. Kinetic studies of thermoset cure reactions: a review. *Polymer*  
47 *Composites.* 1997;18(2):157-68.
- 48 [45] Vyazovkin S, Sbirrazzuoli N. Isoconversional kinetic analysis of thermally stimulated processes in  
49 polymers. *Macromolecular Rapid Communications.* 2006;27(18):1515-32.
- 50 [46] Bilyeu B, Brostow W, Menard KP. Epoxy thermosets and their applications. III. Kinetic equations  
51 and models. *J Mater Ed.* 2001;23:189-97.
- 52 [47] Prime RB. CHAPTER 5 - Thermosets. In: Turi EA, editor. *Thermal Characterization of Polymeric*  
53 *Materials*: Academic Press; 1981. p. 435-569.
- 54 [48] Vyazovkin S. Handbook of thermal analysis and calorimetry: Recent advances, techniques and  
55 applications. In: Brown ME, Gallagher PK, editors. *Amsterdam: Elsevier*; 2011.

- 1 [49] Xia L, Zuo L, Zha S, Jiang S, Guan R, Lu D. Kinetic research on low-temperature cure of epoxy  
2 adhesive. *International Journal of Adhesion and Adhesives*. 2014;50(0):255-64.
- 3 [50] Abadie J. The GRG Method for Nonlinear Programming. In: Greenberg HJ, editor. *Design and*  
4 *implementation of optimization software*. Netherlands: Sijthoff & Noordhoff [International Publishers];  
5 1978. p. 335-63.
- 6 [51] Arrhenius S. On the reaction rate of the inversion of non-refined sugar upon souring. *Z Phys Chem*.  
7 1889;4:226-48.  
8

1 **LIST OF TABLES**

2 Table 1 – Experimental program

3 Table 2 – Geometry measurements of the grooves (average values)

4 Table 3 – Pull-out test results.

5 Table 4 – Regression parameters obtained from model for the evolution of pull-out force

6 Table 5 – Kinetic parameters obtained from autocatalytic isothermal model

7

8

1 **LIST OF FIGURES**

2 Figure 1 – Experimental setup of EMM-ARM tests (exploded view).

3 Figure 2 – Configuration of direct pull-out tests: (a) cross-section of the specimen; (b) view of the  
4 experimental setup.

5 Figure 3 – (a) Evolution of epoxy E-modulus along curing time; (b) setting time *versus* curing  
6 temperature.

7 Figure 4 – Average stress-strain curves obtained by tensile tests

8 Figure 5 – Pull-out force *versus* loaded end slip during curing time at different temperatures: (a) 20 °C;  
9 (b) 30 °C and (c) 40 °C.

10 Figure 6 – Pull-out force *versus* curing time at different temperatures.

11 Figure 7 – (a) Epoxy E-modulus and peak pull-out force along curing time, normalized to 72 hours; (b)  
12 Relationship between epoxy E-modulus and pull-out force.

13 Figure 8 - Curing rate *versus* curing degree: comparison of experimental and autocatalytic model results.

14 Figure 9 - Autocatalytic model: (a) Arrhenius plot of rate coefficient; (b) Curing degree of epoxy  
15 adhesive *versus* equivalent age.

16 Figure 10 – Model-free method applied to epoxy E-modulus: (a) Activation energy *versus* curing degree;  
17 (b) normalized E-modulus of epoxy adhesive *versus* equivalent age (reference: 20 °C).

18 Figure 11 – Model-free method applied to pull-out force: (a) Activation energy *versus* curing degree for  
19 the pull-out force; (b) Pull-out force *versus* equivalent age (reference: 20 °C).

20

21

1 Table 1 – Experimental program

<b>Testing method</b>	<b>Testing Time</b>	<b>20 °C</b>	<b>30 °C</b>	<b>40 °C</b>
Pull-out	4h	-	-	DPT1_4h_T40
	6h	DPT1_6h_T20	DPT1_6h_T30	DPT2_6h_T40
	8h	-	DPT2_8h_T30	DPT3_8h_T40
	9h	DPT2_9h_T20	-	-
	10h	-	DPT3_10h_T30	DPT4_10h_T40
	11h	DPT3_11h_T20	-	-
	12h	-	DPT4_12h_T30	DPT5_12h_T40
	13h	DPT4_13h_T20	-	-
	24h	DPT5_24h_T20	DPT5_24h_T30	DPT6_24h_T40
	72h	DPT6_24h_T20	DPT6_24h_T30	DPT7_24h_T40
7d	DPT7_72h_T20	DPT7_72h_T30	DPT8_72h_T40	
	DPT8_72h_T20	DPT8_72h_T30	DPT9_72h_T40	
EMM-ARM	0h-7d	DPT9_7d_T20	DPT9_7d_T30	DPT10_7d_T40
		DPT10_7d_T20	DPT10_7d_T30	-
Tensile test	7d	EMM1_T20	EMM1_T30	EMM1_T40
		EMM2_T20	EMM2_T30	-
		TT_7d_T20	TT_7d_T30	TT_7d_T40

2

1 Table 2 – Geometry measurements of the grooves (average values)

<b>Curing temperature</b>	<b>Depth [mm]</b>	<b>Width [mm]</b>
DPT_T20	14.13 (2.66%)	5.21 (2.92%)
DPT_T30	15.21 (2.86%)	5.03 (2.17%)
DPT_T40	14.91 (1.48%)	4.94 (3.08%)

2 The values between parentheses are the corresponding coefficients of variation.

1 Table 3 – Pull-out test results.

<b>Curing temperature</b>	<b>Time</b>	<b>Real testing time [h]</b>	<b>Denomination</b>	$F_{t,max}$ [kN]	$\tau_{max}$ [MPa]	$s_{l,max}$ [mm]	<b>Failure mode</b>
20 °C	6h	5.9	DPT1_6h_T20	0.02	0.01	-	FE
	9h	8.9	DPT2_9h_T20	3.07	2.24	0.97	FE
	12h	11.2	DPT3_11h_T20	9.11	6.66	1.64	FE
		12.8	DPT4_13h_T20	13.63	9.96	1.27	FE
	24h	24.5	DPT5_24h_T20	26.27	19.20	0.64	D
		25.9	DPT6_24h_T20	25.76	18.83	0.55	D
	72h	72.2	DPT7_72h_T20	26.17	19.13	0.72	D
		73.2	DPT8_72h_T20	27.24	19.91	0.68	D+SE+CC
	7d	168.6	DPT9_7d_T20	24.50	17.91	0.49	D
		169.9	DPT10_7d_T20	23.87	17.45	0.56	D
30 °C	6h	6.02	DPT1_6h_T30	5.36	3.92	1.55	FE
	8h	7.98	DPT2_8h_T30	12.73	9.31	1.47	FE+D
	10h	10.0	DPT3_10h_T30	17.98	13.14	1.09	FE+D
	12h	12.0	DPT4_12h_T30	21.38	15.63	0.80	FE
		24h	24.2	DPT5_24h_T30	27.88	20.38	0.71
	24h	25.3	DPT6_24h_T30	26.59	19.44	0.75	FE+D
		72h	72.4	DPT7_72h_T30	28.78	21.04	0.89
	72h	73.5	DPT8_72h_T30	25.70	18.79	0.72	D
		7d	168.1	DPT9_7d_T30	26.71	19.52	0.72
	169.5	DPT10_7d_T30	29.83	21.81	0.84	D	
40 °C	4h	4.2	DPT1_4h_T40	2.60	1.90	1.01	FE
	6h	6.1	DPT2_6h_T40	10.46	7.65	1.49	FE
	8h	8.1	DPT3_8h_T40	19.49	14.25	1.12	FE
	10h	10.0	DPT4_10h_T40	22.73	16.62	0.88	FE
	12h	12.0	DPT5_12h_T40	25.02	18.29	0.78	D
		24h	24.0	DPT6_24h_T40	24.94	18.23	0.58
	24h	25.0	DPT7_24h_T40	24.82	18.14	0.62	D
		72h	72.2	DPT8_72h_T40	27.91	20.40	0.56
	72h	73.3	DPT9_72h_T40	27.57	20.15	0.73	D
		7d	168.3	DPT10_7d_T40	27.97	20.45	0.72

2 Notes: FE=cohesive shear failure in epoxy; D=debonding at CFRP-epoxy interface; CC=concrete cracking;

3 SE=splitting of epoxy.

4

1 Table 4 – Regression parameters obtained from model for the evolution of pull-out force

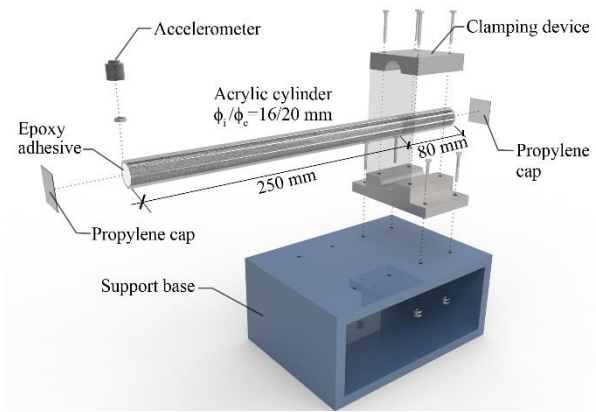
$T_{\text{cure}}$	$F_{\text{ult}}$ [kN]	$\lambda$	$\beta$	$R^2$
20 °C	25.45	14.275	3.374	0.982
30 °C	27.76	9.585	3.058	0.972
40 °C	27.82	7.312	3.012	0.969

2

1 Table 5 – Kinetic parameters obtained from autocatalytic isothermal model

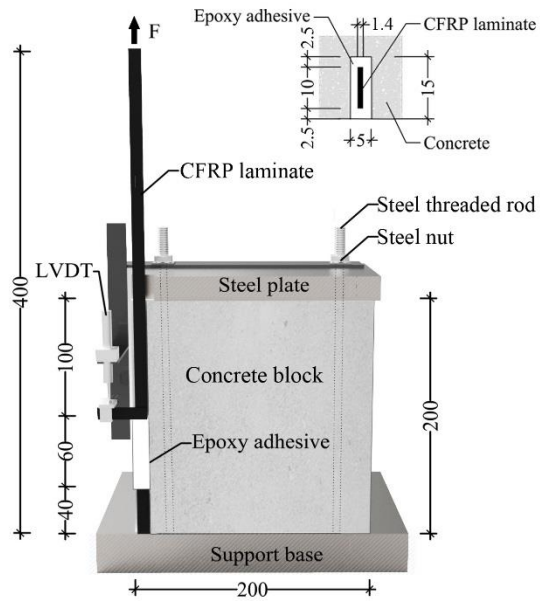
<b>Denomination</b>	<b>m</b>	<b>n</b>	<b>k</b>	<b>R<sup>2</sup></b>	<b>E<sub>a</sub> [kJ/mol]</b>	<b>A [min<sup>-1</sup>]</b>
EMM1_T20	0.672	1.873	11.455	0.839		
EMM2_T20	0.658	1.799	11.848	0.936	↑	↑
EMM1_T30	0.864	2.072	25.729	0.971	34.55	57192529545
EMM2_T30	0.837	1.969	25.316	0.975	↓	↓
EMM1_T40	0.875	1.986	25.969	0.963		

2

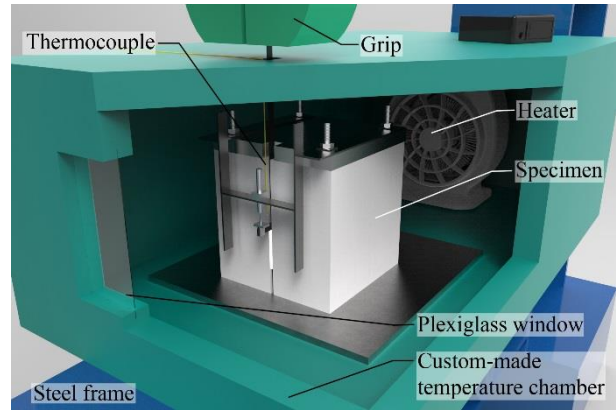


1

2 Figure 1 – Experimental setup of EMM-ARM tests (exploded view).

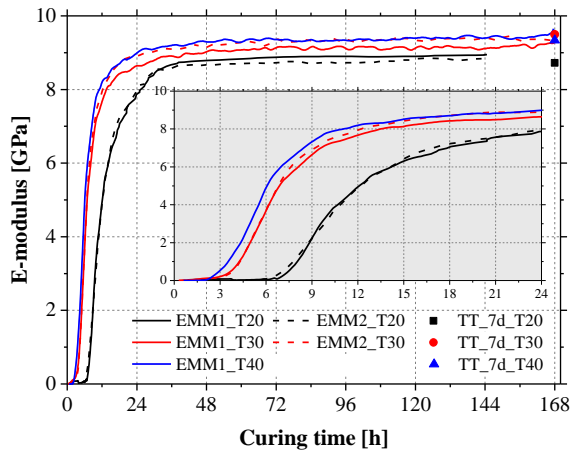


(a)

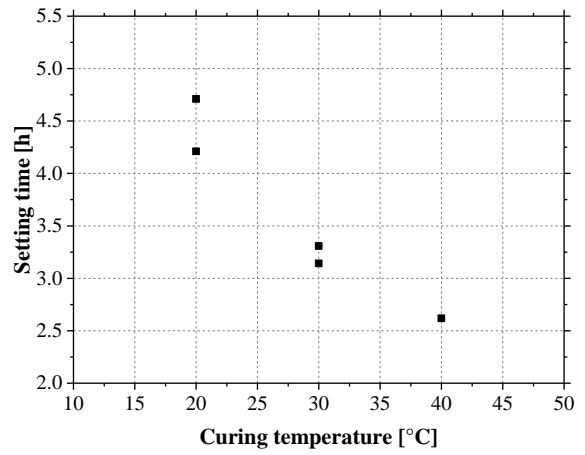


(b)

- 1 Figure 2 – Configuration of direct pull-out tests: (a) cross-section of the specimen; (b) view of the
- 2 experimental setup.

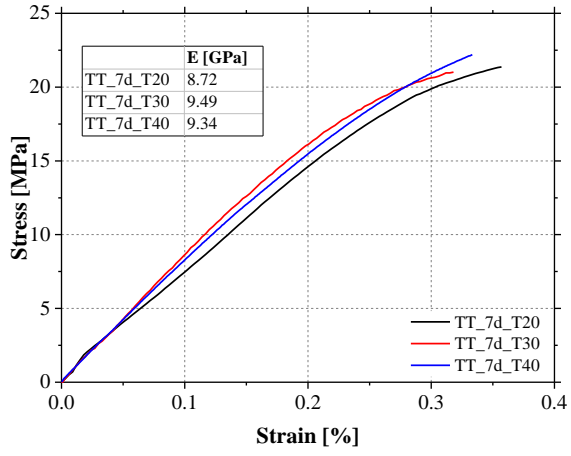


(a)



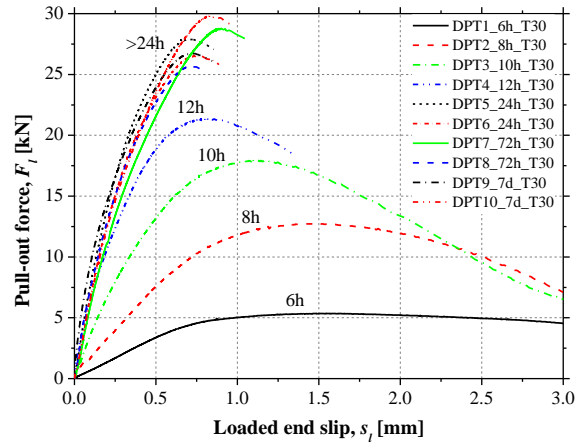
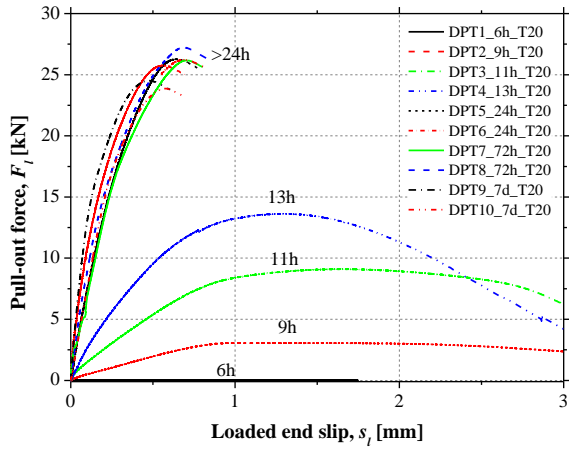
(b)

- 1 Figure 3 – (a) Evolution of epoxy E-modulus along curing time; (b) setting time *versus* curing
- 2 temperature.



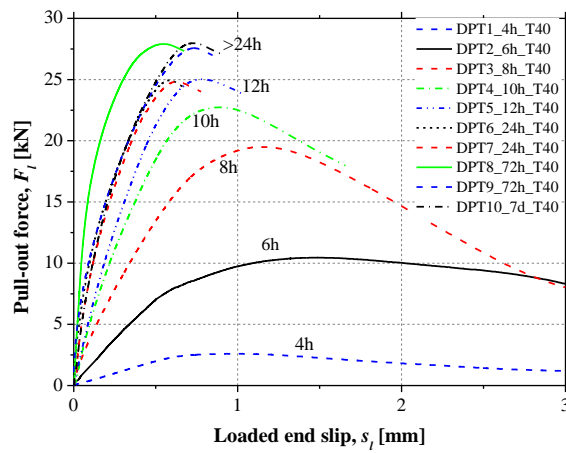
1

2 Figure 4 – Average stress-strain curves obtained by tensile tests



(a)

(b)

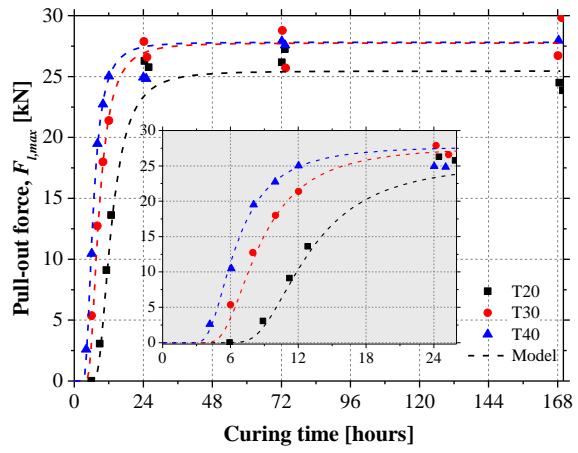


(c)

1 Figure 5 – Pull-out force *versus* loaded end slip during curing time at different temperatures: (a) 20 °C;

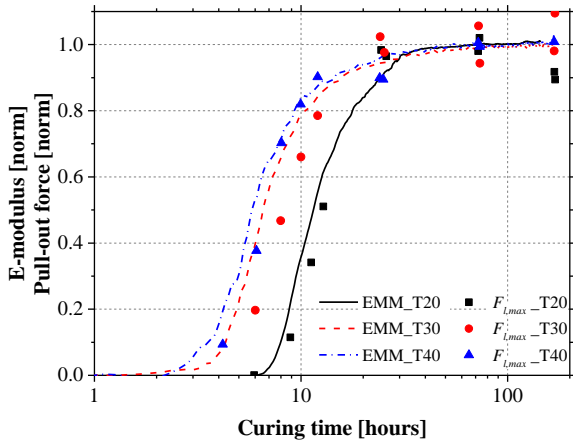
2 (b) 30 °C and (c) 40 °C.

3

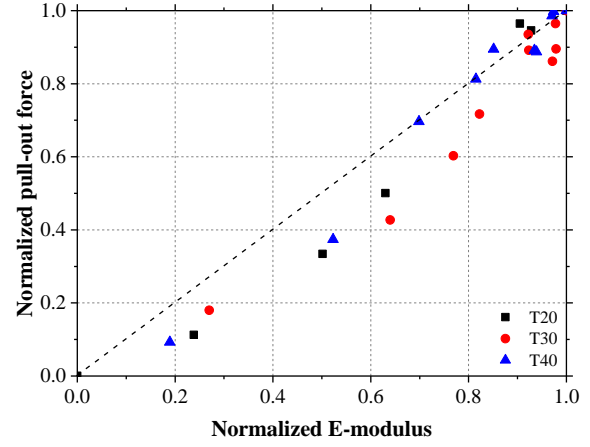


1

2 Figure 6 – Pull-out force *versus* curing time at different temperatures.

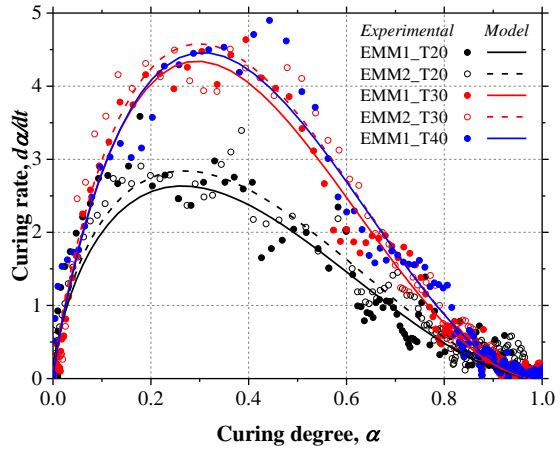


(a)



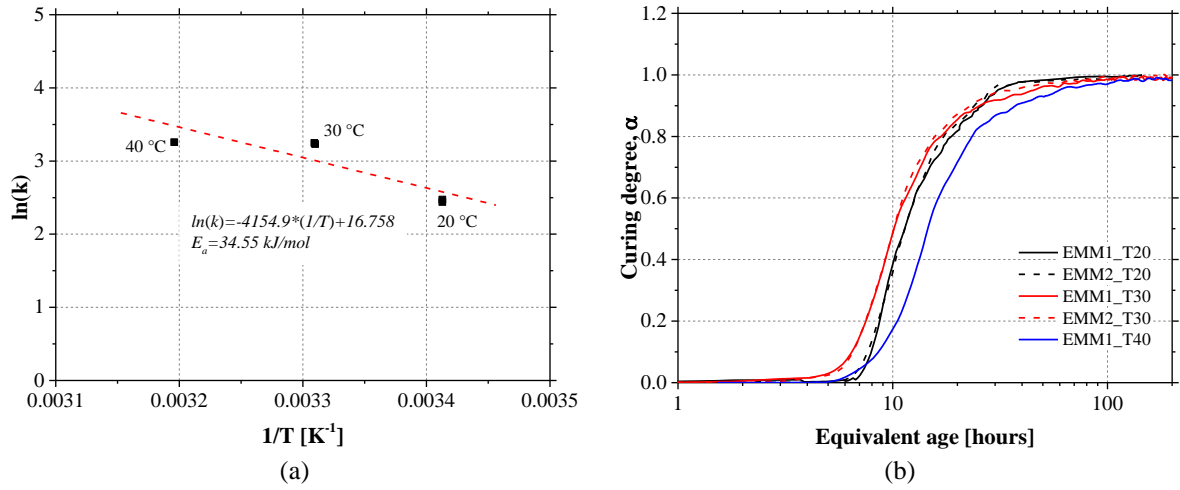
(b)

- 1 Figure 7 – (a) Epoxy E-modulus and peak pull-out force along curing time, normalized to 72 hours; (b)
- 2 Relationship between epoxy E-modulus and pull-out force.

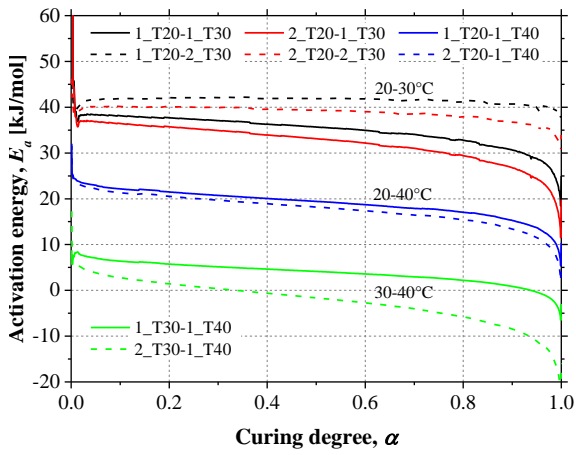


1

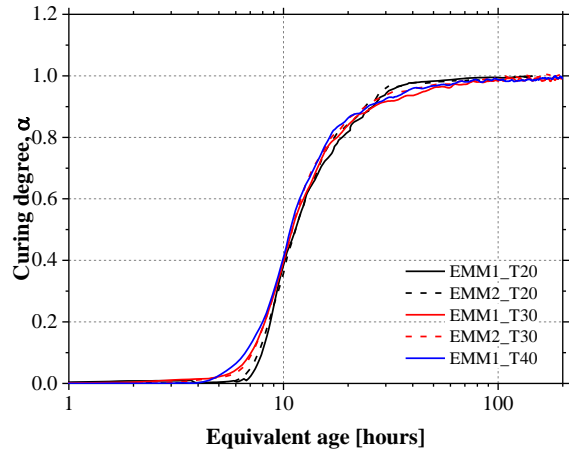
2 Figure 8 - Curing rate *versus* curing degree: comparison of experimental and autocatalytic model results.



1 Figure 9 - Autocatalytic model: (a) Arrhenius plot of rate coefficient; (b) Curing degree of epoxy  
 2 adhesive *versus* equivalent age.

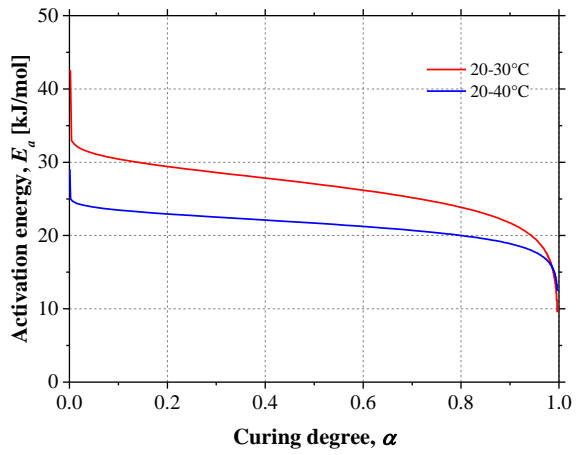


(a)

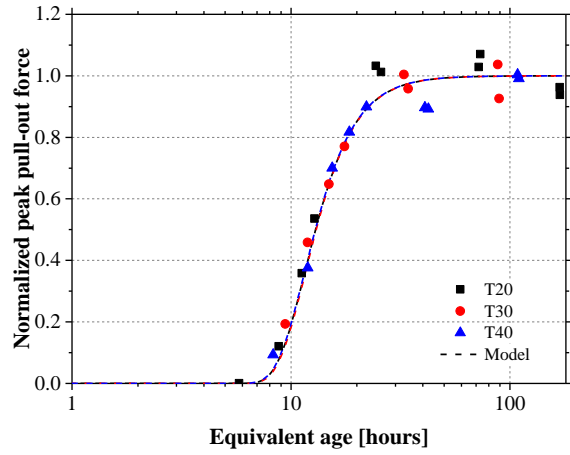


(b)

- 1 Figure 10 – Model-free method applied to epoxy E-modulus: (a) Activation energy *versus* curing degree;
- 2 (b) normalized E-modulus of epoxy adhesive *versus* equivalent age (reference: 20 °C).



(a)



(b)

- 1 Figure 11 – Model-free method applied to pull-out force: (a) Activation energy *versus* curing degree for
- 2 the pull-out force; (b) Pull-out force *versus* equivalent age (reference: 20 °C).